Riblet Drag at Flight Conditions

Michael J. Walsh,* William L. Sellers III,† and Catherine B. McGinley‡
NASA Langley Research Center, Hampton, Virginia

This paper describes perforated and nonperforated riblet tests on the fuselage of a modified Learjet model 28/29 twin-engine business jet at Reynolds numbers of 1.0–2.75 × 10⁶/ft and Mach numbers of 0.3–0.7. Drag reductions of the order of 6% at nondimensional wall spacings of 12 were obtained using boundary-layer rakes and direct drag balances. At the measurement locations, the Reynolds number based on distance was 12–46 × 10⁶. The nondimensional wall spacing for maximum drag reduction was well predicted by low-speed wind-tunnel data, but the maximum drag reduction was lower. The low drag is tentatively ascribed to various instrumentation difficulties and the flowfield on the aircraft. Riblets with 0.010-in. perforations at center spacings of 0.25 in. were found to give the same drag reduction as nonperforated riblets.

Nomenclature

c_f = skin-friction coefficient
D = drag of test surface
D_s = drag of a smooth reference surface
h_p = pressure altitude
M = Mach number
Re = unit Reynolds number per ft
s = physical spacing of riblets, in.
s^+ = spacing of riblets in law of the wall variables
x = distance from the virtual origin of the turbulent boundary layer
α = angle of attack, deg
β = angle of sideslip, deg
θ = momentum thickness, in.

Introduction

ENERGY conservation and the need to maximize aerodynamic efficiency are driving forces behind research into methods of reducing turbulent skin-friction drag on transport aircraft fuselages. Skin-friction reductions as small as 10% can translate into fuel savings of $250 million per year for the airline industry. A passive, retrofittable, easy-to-apply method of skin-friction reduction is to cover the surface with flow-aligned grooves. These grooves, termed "riblets," have heights and spacings that are on the order of the turbulent wall streak and burst dimensions.[1-5] In Ref. 4, symmetric v-groove riblets with spacings and heights of 12–15 wall units were shown to yield drag reductions of 8%. These drag reductions were shown to be relatively insensitive to yaw angles of up to 15 deg, but to vanish for angles of 30 deg.

The work initiated in Ref. 1 has developed into a worldwide research effort as demonstrated by the large number of papers concerning riblets that were presented at a recent conference entitled "Turbulent Drag Reduction by Passive Means" held in London in September 1987.[6] To date, verification of the riblet drag reduction has been reported by Coustols et al.,[7] Sawyer and Winter,[8] Bechert,[9] and Enyutin et al.[10] However, most of the studies have been in low-speed ground facilities and, therefore, have not tested the riblets in one of the environments in which they will be applied – transonic flight conditions. There are currently only two research groups that have reported results for riblet drag reduction at Reynolds and Mach numbers high enough to be directly applicable to transport aircraft. Using boundary-layer rakes to measure changes in the momentum thickness, McLean et al.[11] tested riblets on the wing of a T-33 aircraft. They measured momentum-thickness reductions that were related to skin-friction reductions of approximately 6.5%. Their tests confirmed previous low-speed wind-tunnel tests. The only other transonic work is that of Squire and Saville,[12] who evaluated riblet performance at transonic conditions in a ground facility. They found a 3% drag reduction for riblet sizes on the order of 20 wall units and determined that the drag reduction was a function of the length of the riblet. These results are contradictory to previous low-speed riblet tests. With only one experiment providing data on the performance of riblets in a flight environment, the need for further tests at these conditions was quite obvious.

The purpose of the present investigation was to provide data on riblet performance applicable to transport aircraft fuselages using direct drag and boundary-layer rake measurements. The aircraft fuselage provided a test surface with nearly zero pressure gradient and flow angularity. The present investigation was initiated to provide an independent verification of riblet performance at flight conditions and to clarify the optimum riblet scaling at high Reynolds numbers.

Aircraft, Instrumentation, and Test Surfaces

The test aircraft was a modified Gates Learjet model 28/29 twin-engine business jet. Figure 1 indicates the overall dimensions of the aircraft. The aircraft was flown by NASA Langley Research Center pilots.

An onboard instrumentation system was mounted on a pallet in the airplane baggage compartment area. The data system consisted of both PCM (104 kilobits/s; 217 channels) and FM (narrow and wide band) recording systems. The FM recording system was not used for the present tests. The PCM digital data system was capable of recording 192 pressure measurements and 25 basic airplane performance measurements.

The riblet test surfaces were vinyl sheets with adhesive backing. The individual riblet sheets, which were 12-in. wide and 36-in. long, were overlapped, cut, and butted together to make as long a test panel as required. The riblet sheets were applied to the aircraft by wetting the adhesive side of the riblet with a soapy water solution. The soap solution essentially neutralized the adhesive, allowing the film to be placed on a surface and moved to the proper position. A squeegee was then used to remove the water trapped between the riblet sheet and the surface. Since air bubbles would explode when the aircraft was taken to altitude, extreme care was used to remove them. The

Presented as Paper 88-2554 at the AIAA 6th Applied Aerodynamics Conference, Williamsburg, VA, June 6-8, 1988; received July 8, 1988; revision received Feb. 1, 1989.

*Leader, Turbulent Drag Reduction Group, Viscous Flow Branch.
†Research Scientist, Analytical Methods Branch. Senior Member AIAA.
‡Research Scientist, Viscous Flow Branch.

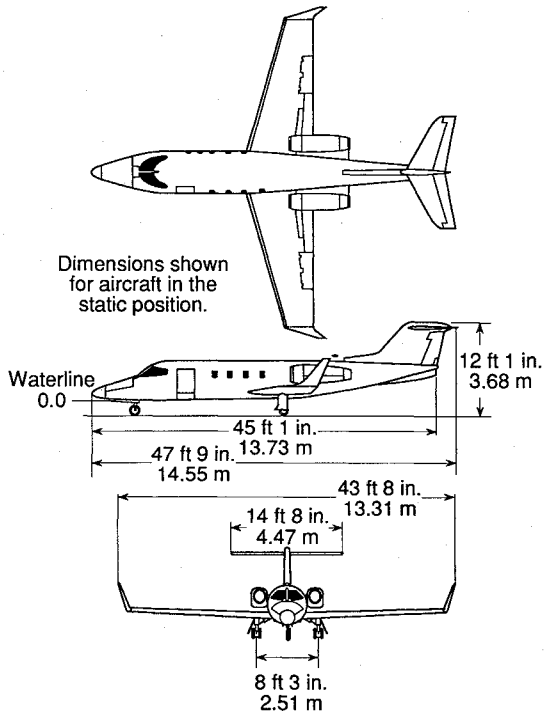

Fig. 1 Overall dimensions of the test aircraft.

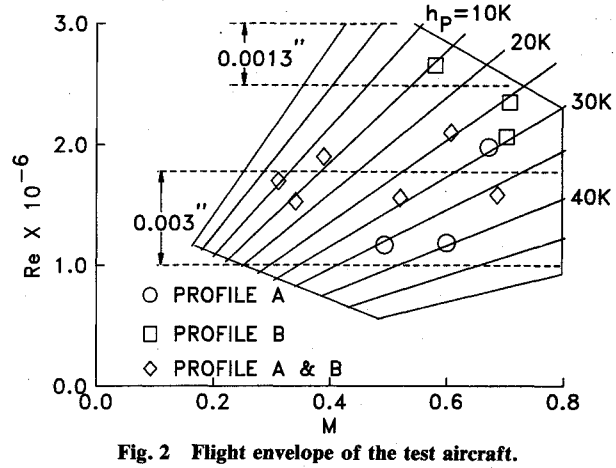

Fig. 2 Flight envelope of the test aircraft.

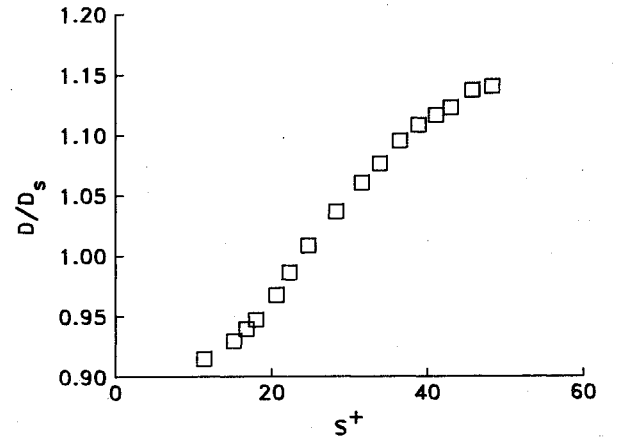

Fig. 3 Optimum riblet determined in low-speed wind-tunnel tests.

riblet sheets were initially applied to a smooth plastic film and then the combined film was applied to the side of the aircraft. This procedure was required so that the test film could be easily removed from the aircraft surface after testing. A paint-type sealer was used at the leading edge of the riblet sheets to insure that the leading edges would not delaminate during the flight and to provide a gradual ramp for the flow at the surface rather than a sudden step.

The riblet geometries tested were symmetric v-grooves with relatively sharp peaks and valleys: one having a spacing and height of 0.0013 in. and one having a spacing and height of 0.003 in. These were the same geometries tested by McLean et al.[11] Since pressurized aircraft cabins leak, porous riblets that diffuse the leakage from joints and rivets will be required for future applications on transport aircraft. Therefore, several porous riblets were also examined in the present tests to determine the effects of perforations on the riblet drag reduction. The effect of leakage through the holes was not examined. The present tests examined riblets with 0.020- and 0.010-in. perforations on center spacings of 0.25 in.

For the majority of the flights, the leading edge of the riblet test panel was aligned with the forward part of the aircraft wind screen, approximately 6.2 ft aft of the aircraft nose. The length of the front test panel was 5.83 ft and the width was 1.0 ft. There were two test-panel locations (upper and lower) on the aircraft, one directly above the other. One of the test-panel locations was always used as a clean or smooth reference surface. To insure that the riblet performance was not dependent on the panel location, the drag-reduction performance was evaluated for riblets in both the upper and lower panel locations.

The drag-reduction performance was determined by boundary-layer rake and direct drag measurements. Two 24-tube boundary-layer rakes were mounted so that the probe tips were located 3.25 in. downstream of the trailing edges of the upper and lower test panels. In the front rake location, the lower and upper rakes were 10.75 and 22.75 in. above the zero waterline. The zero waterline for the aircraft is indicated in Fig. 1. The probe tips were approximately 12 ft from the nose of the aircraft. The resulting velocity profiles were integrated to determine the momentum thickness measured by the rakes. Lower momentum thickness at the rake location was an indication of drag reduction. A momentum balance over the riblet test panel was then used to estimate skin-friction reductions.

The drag balances used in this test were self-nulling devices. Details of their general design can be found in Ref. 13. Specifically for this test, the 2-in.-diam, flush-mounted sensing element was shaped to match the fuselage curvature. When riblet film was applied to the balances, a surgical knife was used to cut out the film around the circular sensing element so that the sensing area was free floating. The full-scale range of the drag balances was set at 10 g. Two drag balances were mounted on the aircraft fuselage 17 ft from the nose of the aircraft, 3.6 ft in front of the wing fuselage junction, and 5.0 ft behind the front rakes. The lower drag balance was 12 in. above the zero waterline, and the upper drag balance was 21 in. above the zero waterline. When the drag balances were mounted on the aircraft, the boundary-layer rakes were installed in the front fuselage location. For several of the flights, the boundary-layer rakes were interchanged with the drag balances to measure the boundary-layer profile at the aft location. Limitations on the penetration of the aircraft fuselage did not permit the use of the drag balances at the front rake locations.

Test Conditions

The flight envelope for the test aircraft is shown in Fig. 2. During the tests, the aircraft was operated at pressure altitudes of 10,000–42,000 ft and Mach numbers ranging from 0.3–0.7. The two riblet geometries tested were selected to provide optimum drag reduction at two different locations in the aircraft's flight envelope. The optimum drag reduction areas for each geometry are indicated by the dashed lines in Fig. 2. Figure 3 shows the drag-reduction performance of a symmetric v-groove riblet as determined in low-speed wind-tunnel tests.[4] The optimum drag reduction found in Ref. 4 was approximately 8% and occurred for a nondimensional riblet height

and spacing of 12–15 wall units. The nondimensional spacing is determined by the following equation:

$$s^+ = sRe\sqrt{c_f/2} \tag{1}$$

The skin-friction coefficient can be estimated from the following equation from Ref. 14:

$$c_f = 0.0576(Rex)^{-0.2} \tag{2}$$

where x is the distance from the origin of the turbulent boundary layer, assumed to be at the aircraft nose for these initial computations. Equations (1) and (2) were used to predict where the 0.0013- and 0.003-in. riblets would given an 8% drag reduction in the aircraft flight envelope. A total of 12 Reynolds and Mach number conditions were selected to cover the aircraft flight envelope. The aircraft could not carry enough fuel to complete the 12 test conditions in one flight. Therefore, the test conditions were divided into two flight profiles (A and B). To verify repeatability, several of the conditions from profile A were retested in profile B. The Reynolds and Mach number for each test condition are shown in Fig. 2. Each profile contained nine different altitude and speed combinations. Since the expected changes in skin friction were small, special emphasis was placed on repeatability. Therefore, as well as having some duplicate flight conditions between the profiles, certain important points were duplicated during each flight. Data were taken at each test condition for a period of 2 min once the flight parameters had stabilized.

Discussion of Results

As was discussed earlier, two measurement techniques were used to evaluate riblet drag-reduction performance: direct drag and boundary-layer rake pitot measurements. The momentum thickness was calculated from the velocity profiles measured by the boundary-layer rakes. Since the forces measured on the drag balance were less than 4 g and the momentum-thickness changes corresponding to an 8% skin-friction reduction were approximately 3%, extreme care in instrumentation calibration and utmost repeatability of the aircraft flight parameters were required to produce precision data. An analysis of the drag-balance data indicated that the drag-balance output was sensitive to the angle of attack α, the Mach number M of the aircraft, and the drag-balance temperature. The drag-balance temperature was measured using a temperature sensor mounted inside the drag balance. Figure 4 shows the drag-balance output for a typical test condition as a function of α, M, and the temperature-sensor voltage of the drag balance. The data shown in Fig. 4 indicate that α varied by 0.6 deg, M varied by 0.005, and the temperature-sensor voltage varied by 0.005 V (1 deg). These changes in flight parameters corresponded to a 5.3% variation in the output of the drag balance.

To reduce the scatter and error in the determination of the net drag, a least-squares fit was made of each data set in Fig. 4 so that the drag could be evaluated at selected α, M, and drag-balance temperature. The solid lines in Fig. 4 are the least-squares fit the drag data as a function of the single variable shown on the x axis. There is a considerable amount of scatter about each fit. The scatter indicates that the drag-balance output is sensitive to other parameters in addition to the parameter indicated on the x axis.

A multiple regression analysis (MRA) procedure was developed to better fit the data of Fig. 4. The MRA technique uses conventional matrix methods[15] to fit a regression model of the form

$$D = \eta_0 + \eta_1\alpha + \eta_2\beta + \eta_3 M \tag{3}$$

where η_i, $i = 0, 3$, are the regression coefficients. Figure 5 compares the difference between the actual drag data with the

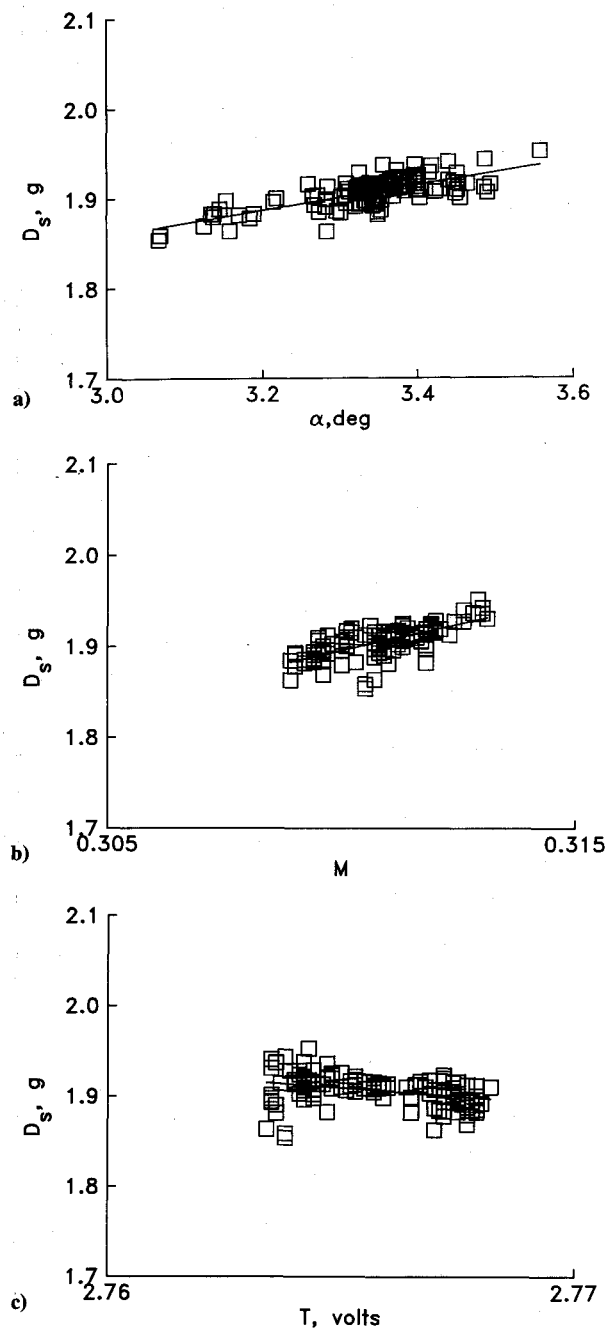

Fig. 4 Comparison of drag-balance data with least-squares fit: a) angle of attack; b) Mach number; and c) drag-balance temperature.

least-squares fit of Fig. 4 and the MRA fit using the same data. Figure 5 indicates that the multiple linear regression provides a better fit of the measured data and reduces the scatter about the fit by one-half. The MRA fits were then used to determine the drag-balance output at a nominal value of α, M, and drag-balance temperature. This is the value of drag that was used to compare the different flight conditions. The nominal values of α, M, and drag-balance temperature were always selected to be within the data range for each flight condition, i.e., the nominal Mach number was always between the minimum and the maximum Mach number obtained for each data set. The drag data obtained at identical test conditions but during different flights were repeatable within 1–2% when reduced using the above procedure.

Figure 6 presents the flight drag data from the present tests in terms of D/D_s, where D is the drag of a riblet surfce and D_s is the drag of the clean aircraft fuselage. The riblet drag data were obtained for the case where the riblet film was placed on the drag balance only. This test procedure could be used

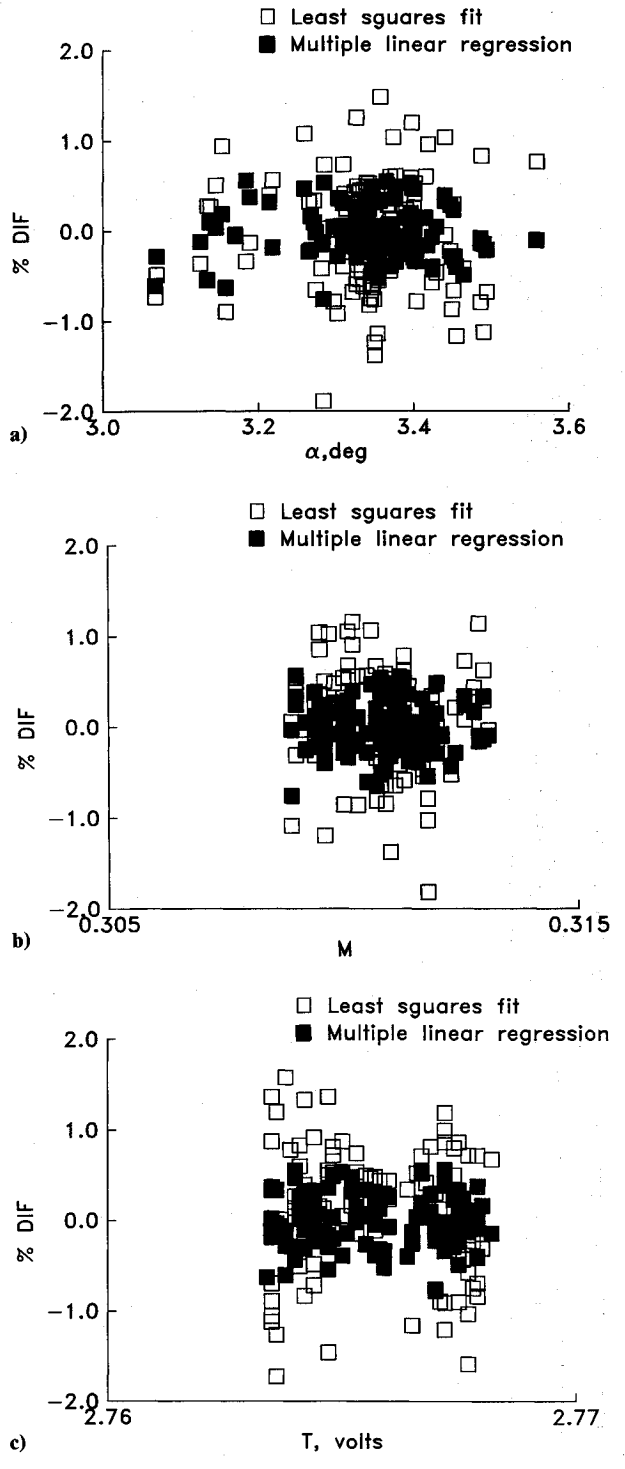

Fig. 5 Comparison of drag-balance data with least-squares fit and multiple linear regression fit: a) angle of attack; b) Mach number; and c) drag-balance temperature.

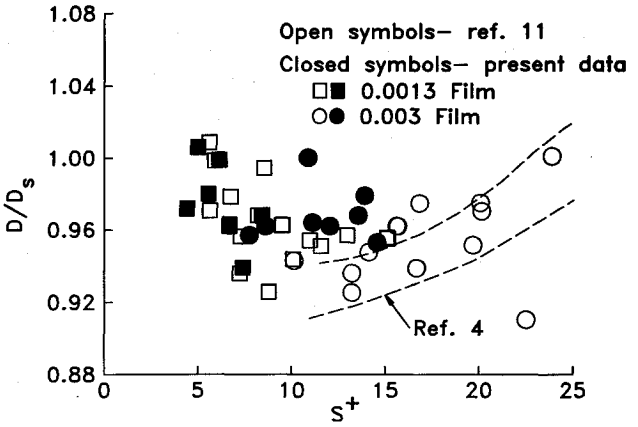

Fig. 6 Riblet flight drag-balance data.

because the riblets modify the near-wall structure of the turbulent boundary layer, affecting eddies on the order of 100 wall units. It is estimated that the riblets on the aircraft became effective within one boundary layer or approximately 2 in. The edge of the sensing area of the drag balance is 2.75 in. from the start of the riblet film. Therefore, the riblets are effective over the sensing element of the drag balance. Figure 6 also shows the flight data of McLean et al.[11] and a band representing the low-speed riblet data of Ref. 4. The present 0.0013 riblet film data seem to agree with the data of Ref. 11, but the drag for the 0.003 riblet data are slightly higher. The level of drag reduction and the agreement with previous data will be discussed further after the presentation of the boundary-layer rake data.

There are two problems in using boundary-layer rake data to indicate changes in drag: 1) relating changes in the measured velocity profile to skin friction, and 2) the repeatability of the data. The initial test plan was to place the riblet test panels between the two longitudinal rake positions and to measure the profile at the front and aft locations. Then, differences in the boundary-layer properties between the forward and aft rake locations could be related to skin-friction changes by the following equation

$$c_f = \tfrac{1}{2}(\mathrm{d}\theta/\mathrm{d}x) \tag{4}$$

Equation (4) is valid for a two-dimensional, zero pressure-gradient flow. The initial flight data indicated that the data for the front rake were repeatable, and there was no reason to suspect any unusual flow angularity at this location. However, problems with data repeatability at the back rake location led to a suspicion that the flow at this location was slightly three-dimensional, probably due to the flowfield characteristics of the wing/fuselage junction. Therefore, the proposed test-panel location was moved forward to a fuselage location ahead of the forward rakes where the flow was nominally two-dimensional.

Because of limitations on fuselage penetrations and test time, a new rake location could not be made ahead of the new test-panel location. The momentum thickness ahead of the test panel was estimated so that changes in the momentum thickness at the front rake position could be related to changes in skin friction. The procedure used to estimate the momentum thickness ahead of the test panel required the determination of the most probable location for boundary-layer transition. Seven inches from the nose of the aircraft was a junction between the nose cap and the fuselage. This junction had a mismatch between the nose cap and the fuselage that resulted in a 1/16-in. backward-facing step. Calculations estimated that the roughness Reynolds number was 5.8×10^3 and the momentum-thickness Reynolds number was 4.5×10^2. It is generally accepted that a roughness Reynolds number of 4×10^2 will trip the boundary layer and a momentum-thickness Reynolds number greater than 2×10^2 will maintain turbulent flow. Therefore, there was sufficient evidence that the boundary layer was turbulent after the nose-cap junction. This junction was then used as the virtual origin for the turbulent boundary layer. The following equation from Ref. 14 relates the momentum thickness to the distance from the virtual origin for a two-dimensional turbulent boundary layer:

$$\theta = 0.036x^{0.8}Re^{-0.2} \tag{5}$$

The momentum thickness at the leading edge of the test panel was estimated by using the growth rate of θ as determined by

Eq. (5) and extrapolating from the measured momentum thickness at the forward rake location. Then Eq. (4) was used to relate the momentum-thickness changes to changes in skin friction. It was estimated that a ±7 in. uncertainty in the virtual origin would relate to a ±0.5% change in the calculated drag reduction.

The momentum thickness obtained from integration of the velocity profiles was found to be sensitive to the flight parameters α, β, and M, where β is the side-slip angle of the aircraft in degrees. A multiple least-squares-fit procedure, similar to the one presented earlier in the interpretation of the drag-balance data, was used to adjust the measured velocities of the rake pitot tubes to nominal values of the flight parameters α, β, and M. The ratio of the upper and lower panel momentum thickness for identical test conditions but different flights were then found to be repeatable within 1–1.5%. Therefore, the drag-reduction performance of the riblets was interpreted in terms of changes in the ratio of the momentum thickness of the two test panels where one panel was always a clean reference.

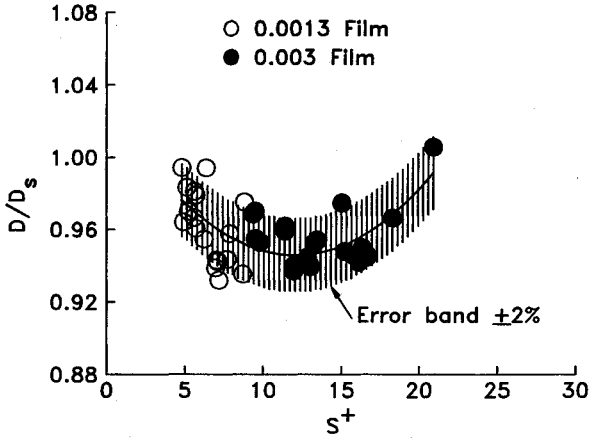

Fig. 7 Drag determined by front boundary-layer rakes.

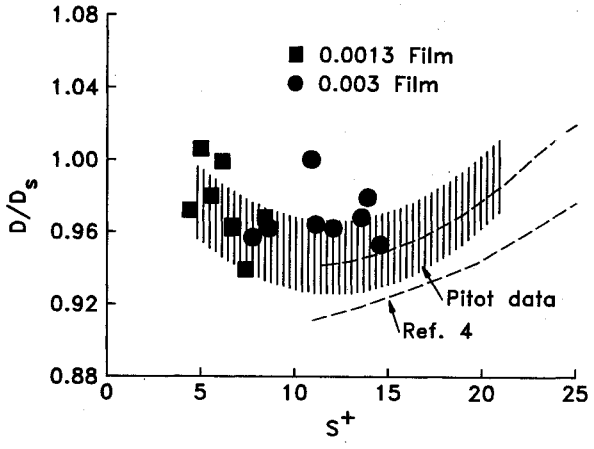

Fig. 8 Comparison of drag balance and pitot rake data.

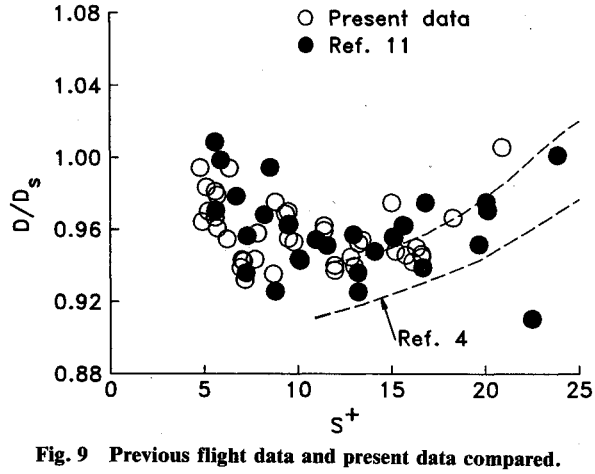

Fig. 9 Previous flight data and present data compared.

Figure 7 presents the riblet drag-reduction performance determined using the above interpretation of the measured velocity data. The solid line is the least-squares fit of the data, and the hatched area represents the error band. The band of scatter is approximately ±2%, and the maximum drag reduction is approximately 6%. Figure 8 compares the riblet drag-reduction performance measured by the drag balances in the aft fuselage location to that measured by the boundary-layer rakes in the front fuselage location. The drag balance and boundary-layer rake data are in fair agreement; however, the drag-balance data for the 0.003-in. riblet indicate slightly lower drag reduction than the rake data. Figure 9 compares the present data for riblet drag reduction to the data of McLean et al.,[11] who found a 6.5% drag reduction at approximately the same s^+ as the present tests.

The pitot and drag-balance data are both sensitive to flow angularity and pressure gradient. Since the two sets of instrumentation are in different locations on the fuselage, the measurements will be affected by different flow angles and pressure gradients. The VSAERO (Vortex Separation Aerodynamics Program) computer code was used to examine the flow angularity and the pressure distribution on the aircraft. This code is a surface singularity panel method, which uses quadrilateral panels to represent arbitrary three-dimensional configurations. The code can calculate streamlines and pressure distributions. Reference 16 contains the details of VSAERO. The computations indicated that the pressure variation along the fuselage was small. Figure 10 shows the fuselage of the Learjet and the calculated streamlines for an $\alpha = 4.9$ deg and a Mach number of 0.5. The test panel and the instrumentation locations are marked on the figure. At the front rake location, the streamlines are essentially parallel to the waterline of the aircraft; however, at the aft drag balance and rake location the flow angles are 6 and 9 deg at the lower and upper balance locations, respectively. McLean et al.,[11] found that a deliberate yaw angle of 15 deg decreased the riblet drag reduction from 6.5% to aproximately to 3%.

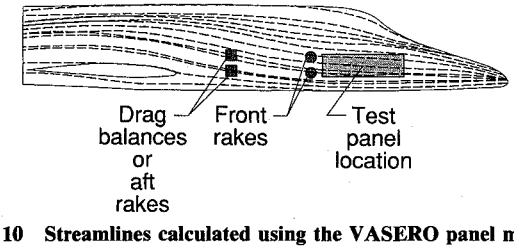

Fig. 10 Streamlines calculated using the VASERO panel method.

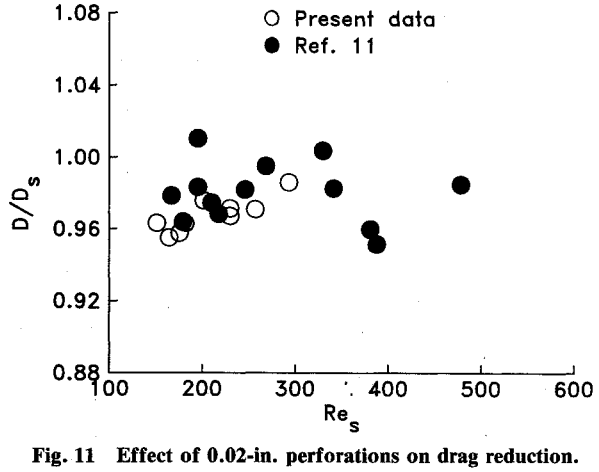

Fig. 11 Effect of 0.02-in. perforations on drag reduction.

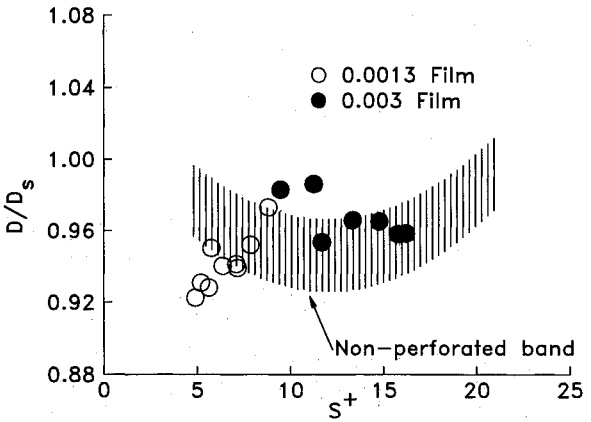

Fig. 12 Effect of 0.01-in. perforations on drag reduction.

Based on the effect of yaw, one would expect the indicated drag-reduction performance determined by the drag balances to be somewhat low. Therefore, it is reasonable that the flow angularity at the aft station could explain any reduction in riblet performance as indicated by the drag-balance data.

Film applied to the pressurized fuselages of transport aircraft must be perforated so that the fuselage leakage through rivet holes can be released. McLean et al.[11] tested porous riblet film with 0.020-in. perforations spaced 0.25 in. and found that the drag reduction was one-half that of nonperforated film. Figure 11 shows that the present data obtained for 0.0013-in. riblets with 0.020-in. perforations confirmed the results of Ref. 11. Figure 12 indicates the results for a 0.010-in. laser-perforated riblet film. The perforations are spaced at 0.25 in. Both the 0.0013- and 0.003-in. riblet films were tested with the 0.010-in. perforations. The data in Fig. 12 indicate that the 0.010-in. perforations are small enough not to degrade the riblet drag reduction. The small increase in drag reduction at $s^+ = 5$ is felt to be within the scatter of the data.

Concluding Remarks

The present test confirmed riblet drag reduction at flight conditions. The present drag reductions are estimated to be about 6%, approximately the same level as found in earlier flight tests. The present riblet performance levels were measured by boundary-layer rakes in the front portion of the aircraft fuselage and drag balances in the aft portion of the fuselage. The drag-balance location had flow angles that may have degraded the riblet performance. The front rake data had to be extrapolated forward of the rake position to convert reduced momentum-thickness measurements to reductions in skin friction. This extrapolation procedure may vary somewhat according to the actual location of boundary-layer transition. If the virtual origin of the turbulent boundary layer was actually closer to the nose, the present estimates of riblet performance will be low. Porous riblets with perforations of 0.010 in. and center spacings of 0.25 in. were found to have the same reduction as the nonperforated riblet film.

References

[1]Walsh, M. J. and Weinstein, L. M., "Drag and Heat Transfer on Surfaces with Small Longitudinal Fins," AIAA Paper 78-1161, July 1978.

[2]Walsh, M. J., "Turbulent Boundary-Layer Drag Reduction Using Riblets," AIAA Paper 82-0169, Jan. 1982.

[3]Hooshmand, A., Youngs, R. A., Wallace, J. W., and Balint, J. L., "An Experimental Study of Changes in the Structure of a Turbulent Boundary Layer Due to Surface Geometry Changes," AIAA Paper 83-0320, Jan. 1983.

[4]Walsh, M. J. and Lindemann, A. M., "Optimization and Application of Riblets for Turbulent Drag Reduction," AIAA Paper 84-0347, Jan. 1984.

[5]Nitsche, P., *Experimentelle Undersuchung Turbulent en Stroenung in Glatten und Loenasyerillten Romen*, Max-Planck Institut fuer Stromungsforschung, Goettingen, Germany, 1983.

[6]*Proceedings of the Conference on Turbulent Drag Reduction Conference by Passive Means*, Royal Aeronautical Society, London, England, Sept. 1987.

[7]Coustols, E., Cousteix, J., and Belanger, J., "Drag Reduction Performance on Riblet Surfaces and Through Outer Layer Manipulators," *Proceedings of the Conference on Turbulent Drag Reduction Conference by Passive Means*, Royal Aeronautical Society, London, England, Sept. 1987.

[8]Sawyer, W. G. and Winter, K. G., "An Investigation of the Effect of Turbulent Skin Friction of Surfaces with Streamwise Grooves," *Proceedings of the Conference on Turbulent Drag Reduction Conference by Passive Means*, Royal Aeronautical Society, London, England, Sept. 1987.

[9]Bechert, D. W., "Experiments on Three-Dimensional Riblets," *Proceedings of the Conference on Turbulent Drag Reduction Conference by Passive Means*, Royal Aeronautical Society, London, England, Sept. 1987.

[10]Enyutin, G. V., Lashkov, Y., Samoilova, N. V., Fadeev, I. V., and Shumikina, E. A., "Experimental Investigation of the Effect of Longitudinal Riblets on the Friction Drag of a Flat Plate," *Fluid Dynamics*, Vol. 23, March–April 1987, pp. 284–289.

[11]McLean, J. D., George-Falvy, D. N., and Sullivan, P. P., "Flight Test of Turbulent Skin-Friction Reduction by Riblets," *Proceedings of the Conference on Turbulent Drag Reduction Conference by Passive Means*, Royal Aeronautical Society, London, England, Sept. 1987.

[12]Squire, L. C., and Saville, A. M., "Some Experiences of Riblets at Transonic Speeds," *Proceedings of the Conference on Turbulent Drag Reduction Conference by Passive Means*, Royal Aeronautical Society, London, England, Sept. 1987.

[13]Tcheng, P. and Supplee, F. H., "A Flight Balance for Skin-Friction Measurements," 12th International Congress on Instrumentation in Aerospace Simulation Facilities, Williamsburg, VA, June 1987.

[14]Schlichting, H. *Boundary-Layer Theory*, 6th ed., McGraw-Hill, New York, 1968.

[15]Draper, N. R. and Smith, H., *Applied Regression Analysis*, Wiley, New York, 1966, pp. 104–123.

[16]Maskew, B., "Prediction of Subsonic Aerodynamic Characteristics: A Case for Low-Order Panel Methods," *Journal of Aircraft*, Vol. 19, Feb. 1982, pp. 157–163.